

Analysis of the Mechanical Characteristics of a 17-MW-Class High-Temperature Superconducting Synchronous Motor

Ji Hyung Kim · Sail Park · Thanh Dung Le ·
Hyun Chul Jo · Young-Sik Jo · Yoon Hyuck Choi ·
Haigun Lee · Ho Min Kim

Received: 16 June 2014 / Accepted: 22 September 2014 / Published online: 5 October 2014
© Springer Science+Business Media New York 2014

Abstract This paper presents an analysis of the mechanical characteristics of a 17-MW-class high-temperature superconducting (HTS) synchronous motor. The fundamental electromagnetic, structural, and thermal design must be accompanied to maintain the reliability of an HTS rotating machine when designing an HTS synchronous motor with an HTS wire with a high current density instead of a copper wire used in a conventional rotating machine. Therefore, we analyze the structural characteristics from two perspectives using three-dimensional (3D) finite-element analysis for the structural design of a 17-MW-class HTS synchronous motor that is intended to be utilized for ships with electric propulsion.

Keywords Finite-element analysis · High-temperature superconducting synchronous motor · Mechanical characteristic · Mechanical stress

J. H. Kim · S. Park · T. D. Le · H. M. Kim (✉)
Department of Electrical Engineering, Jeju National University,
Jeju 690-756, South Korea
e-mail: hmkim@jejunu.ac.kr

H. C. Jo
School of Electrical and Electronic Engineering,
Yonsei University, Seoul 120-749, South Korea

Y.-S. Jo
Korea Electrotechnology Research Institute,
Changwon 641-120, South Korea

Y. H. Choi · H. G. Lee
Department of Materials Science and Engineering,
Korea University, Seoul 136-713, South Korea

1 Introduction

As part of the efforts to reduce greenhouse gas emissions and improve energy efficiency, the ship propulsion system of high-value-added ships such as luxury cruise ships and warships that are currently being developed will be converted from conventional mechanical propulsion systems to electrical propulsion systems that are combined with superconductivity technology.

A high-temperature superconducting (HTS) motor has several specific advantages. The following are the advantages of using an HTS wire with high current density and zero resistance: (a) it is possible to manufacture motors that have a compact volume and lighter weight; (b) it is possible to achieve low loss and high efficiency by reducing the excitation loss; (c) an air-core stator capable of creating low vibration and noise can be manufactured from nonmagnetic materials; (d) it is possible to achieve efficiency at low loads that is higher than that of conventional machines; and (e) the transient stability according to the load changes can be improved because the synchronous reactance can be reduced by up to 80 % as compared with a conventional synchronous motor. However, an HTS motor should be operated in a cryogenic environment and high magnetic field in order to achieve the above advantages. Accordingly, the design of an HTS motor with high reliability is required by using a comprehensive design procedure that consists of electromagnetic, structural, and thermal designs.

In this study, an analysis of the mechanical stresses has been performed by commercial three-dimensional (3D) finite-element analysis (FEA) software for the electromagnetic design of a 17-MW-class HTS motor in order to ensure the structural safety of each configuring part of the HTS motor, such as the HTS field coils and rotor. For the HTS

Table 1 Design Parameter Specifications of a 17-MW HTS Motor

Design specifications			
Rated output power [MW]		17	
Rated frequency [Hz]		9	
Rated rotation speed [rpm]		180	
Rated output voltage [V]		6600	
Rated torque [N m]		902,340	
Efficiency [%]		96.038	
Synchronous reactance [p.u]		0.34	
Machine volume [m ³]		8.97	
Machine weight [kg]		37,106	
Power factor		1.0	
HTS field coil		Armature winding and stator	
Rated excitation current [A]	91	Phase current [A]	1487
Turns of the field coil	36,264	Number of slots	72
HTS wire length [km]	182.7	Stator coil turns per phase	120
Rotor current density [A/mm ²]	54.35	Stator current density [A/mm ²]	10
Operating temperature [K]	40	Insulating class	F

field coils, the mechanical stress is defined by the electromagnetic Lorentz force, and mechanical stress is determined by the machine torque for the rotor [1].

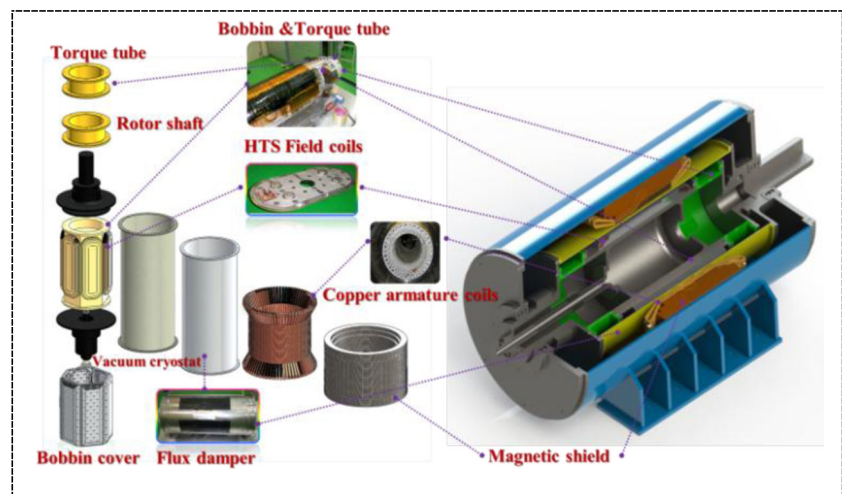
2 Analysis of the Mechanical Characteristics of 17-MW-Class High-Temperature Superconducting Motor

2.1 Structural Design

Table 1 lists the design specifications of the analytical model for a 17-MW-class HTS motor, and the resulting conceptual design to determine the structural safety of the HTS motor is

displayed in Fig. 1. The rotor of the HTS motor is composed of HTS field coils to generate the torque, a torque tube, and a rotating shaft. Torque is delivered from the torque tube to the rotating shaft and from the rotating shaft to the external propellers. Additionally, a flux damper and vacuum insulation layer for electromagnetically protecting the HTS field coil and preventing heat intrusion from areas at room temperature, respectively, are installed. In addition, the air-core stator of the HTS motor consists of armature coils that are wound by conventional copper conductors such as Litz wire, stator supporters manufactured with fiberglass-reinforced plastic (FRP), and a magnetic shield that prevents the rotating magnetic field generated by the three-phase armature coils from leaking to the outside.

Fig. 1 Cross-sectional structure of a 17-MW-class HTS synchronous motor



Starting with the basic design of the HTS motor from a two-dimensional (2D) design code, a 3D FEA program is utilized to optimize the proposed basic design in order to reduce the design errors due to leakage flux at the air gap [1]. The total length of the HTS wire manufactured by Sumitomo Corporation used in the superconducting field coil, which is important for designing the superconducting rotating machine, is approximately 182.7 km. Moreover, the machine efficiency computed by 3D FEA was 96.038 %, which is approximately 1.3 % lower than the 2D design efficiency of 97.35 %. Additionally, the total weight and volume of the HTS motor are 37,106 kg and 8.97 m³, respectively.

2.2 Analysis of the Mechanical Characteristics of the HTS Field Coil

The HTS field coil used for analysis consists of nine layers of double-pancake coils with an insulating plate in between and is shown in Fig. 2. The race-track-type HTS field coils are wound by the way of non-insulating winding method. Furthermore, the specifications of the HTS wire from Sumitomo Corporation used to design the HTS field coils are listed in Table 2. Because of the air-core-type electric machine, more magnetomotive force is needed in the field coil. For this reason, the high magnetic field electromagnetically affects the superconducting field coils. Accordingly, the electromagnetic forces can be strong [2]. Therefore, in order to design an optimal HTS field coil to withstand the mechanical stress caused by Lorentz force, the structural safety of the HTS field coils should be determined with the mechanical stresses and yield strengths of

Table 2 Specifications of the HTS wire

Conductor property	Value
Conductor type	Bi-2223
Thickness [mm]	0.35
Width [mm]	4.6
Critical current [A] @ 77 K, SF	≥ 180
Critical tensile strength [MPa] @ 77 K	270 (longitudinal direction)

the materials used in the HTS wire, insulating plate, and bobbin block as well.

The Lorentz force density F acting on the HTS wire is expressed by

$$F = J \times B, \tag{1}$$

where J is the current density [A/m²], and B is the magnetic flux density [T].

The electromagnetic force in (1) and the mechanical stress generated by the components of the magnetic field vector are conceptually shown in Fig. 3 [3]. From the direction of the superconducting wire width, the Lorentz force caused by the magnetic field in the parallel direction (B_x) creates a radial stress and hoop stress along the curvature.

Additionally, the compressive force acts as a shear stress because of the perpendicular (B_y) magnetic field. The

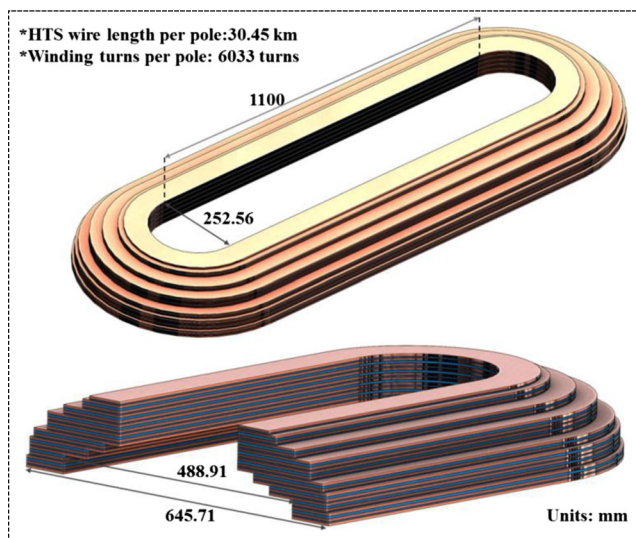


Fig. 2 Schematic view of the HTS coil for the 17-MW-class HTS synchronous motor

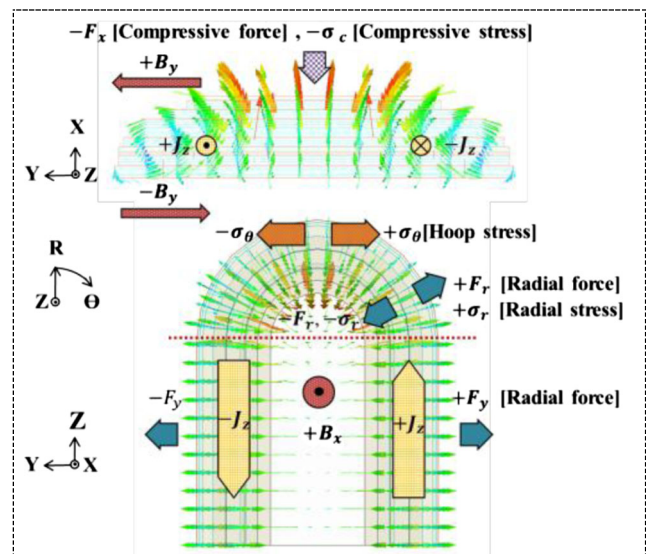
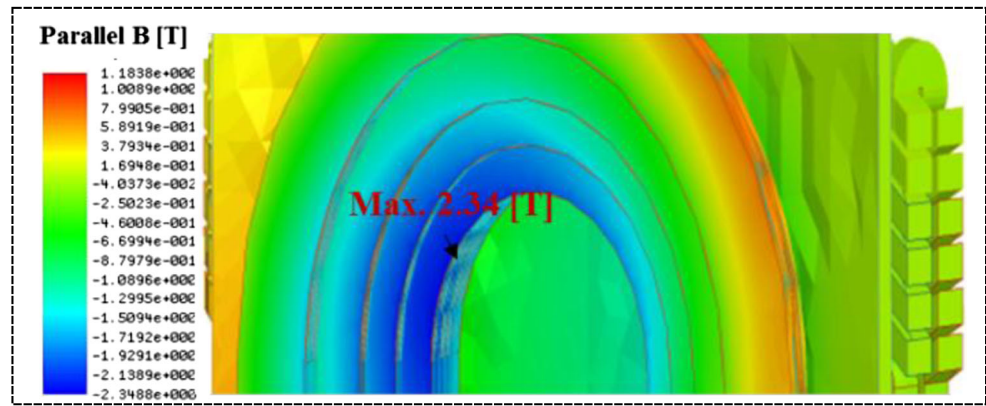


Fig. 3 Diagram of the electromagnetic force and mechanical stress acting on the HTS field coils

Fig. 4 Three-dimensional magnetic-field distribution of the parallel direction (B_x) along the curvature of the HTS field coil



results of the magnetic field distribution analysis during full-load operation show that the maximum value of the parallel magnetic field that determines the Lorentz force is approximately 2.34 T, as shown in Fig. 4.

Figure 5 shows the analysis model for calculating the mechanical stress that occurs in the superconducting field coils, and Table 3 lists the material properties required for

the stress analysis [4, 5]. The results of the mechanical-stress analysis show that the maximum equivalent stress along the curvature of the HTS field coils, which occurs in a single-pancake (SP) coil in the 2nd layer, is 7.46 MPa. By calculating the equivalent stress for fracture or plastic deformation of the structure, the structural safety of the HTS field coils was determined. The mechanical stresses along the curvature of the coils are obtained with the following transformation equations for the plane stress [6, 7]:

$$\sigma_{\text{radial}} = \frac{\sigma_x + \sigma_y}{2} + \frac{\sigma_x - \sigma_y}{2} \cos 2\theta + \tau_{xy} \sin 2\theta \quad (2)$$

$$\sigma_{\text{hoop}} = \frac{\sigma_x + \sigma_y}{2} - \frac{\sigma_x - \sigma_y}{2} \cos 2\theta - \tau_{xy} \sin 2\theta \quad (3)$$

where σ_x and σ_y are the normal stresses acting in the x and y directions, respectively. τ_{xy} is the shear stress acting in the x–y plane, and θ , which has a range from 0 to 180°, is the angle at the point where stress is generated along the curvature of the coils. The stress elements are converted from

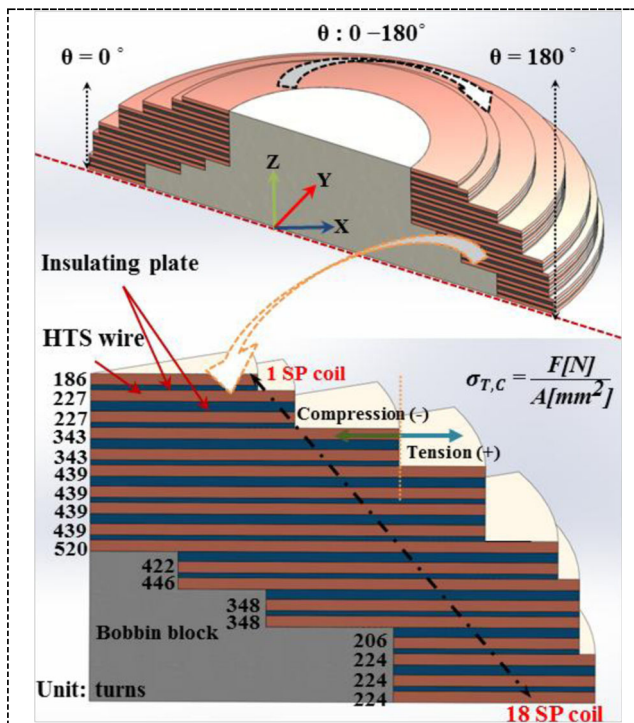
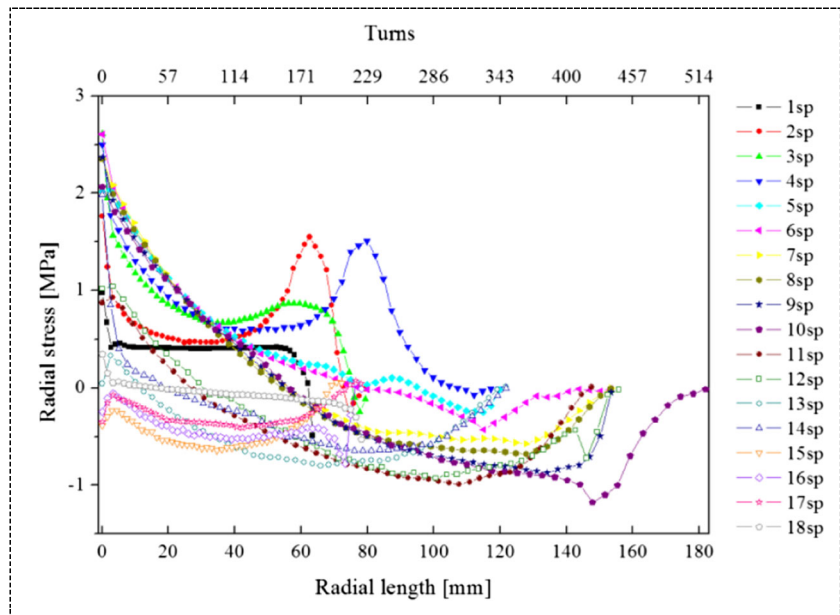


Fig. 5 Overview of the analysis model for the mechanical-stress analysis at the curved parts of the HTS field coils

Table 3 Mechanical Properties of the HTS Field Coil for Structural Analysis

Material	Bi-2223
Young's modulus [GPa]	63.7
Shear modulus [GPa]	26.992
Poisson's ratio	0.18
Tensile yield strength [MPa]	270 (longitudinal) 20–40 (transverse)

Fig. 6 Radial-stress variation at the generated maximum radial stress in the radial direction along the curvature of each SP coil; tension (+)



a Cartesian coordinate system to a cylindrical coordinate system by using (2) and (3).

Figures 6, 7, and 8 show the changes in the mechanical stress that occur in the radial direction along the curvature of each single-pancake (SP) coil. In order to realize the point where the maximum stress is generated, the stress change generated in the radial direction was calculated at the maximum stress point, and Table 4 lists the point of the generated

stress and the maximum radial stress, hoop stress, and compressive stress, which are generated along the curvature of the HTS field coils.

The results of the stress analysis show that a maximum radial stress of 2.7 MPa is generated in the 1st winding of the SP coil of the 5th layer. Its value level is lower than strength values of BSCCO wire in the transverse direction (20–40 MPa) [5]. Additionally, the maximum hoop stress, which

Fig. 7 Hoop-stress variation at the generated maximum hoop stress in the radial direction along the curvature of each SP coil; tension (+)

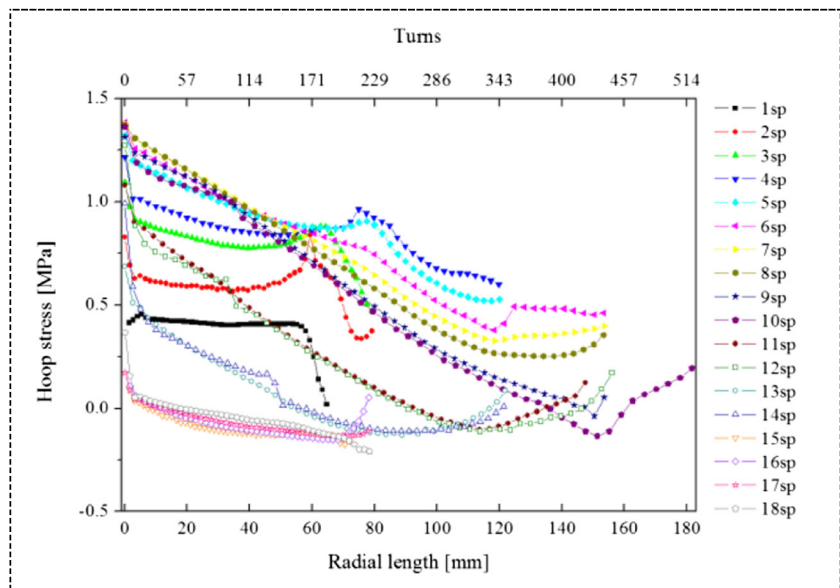
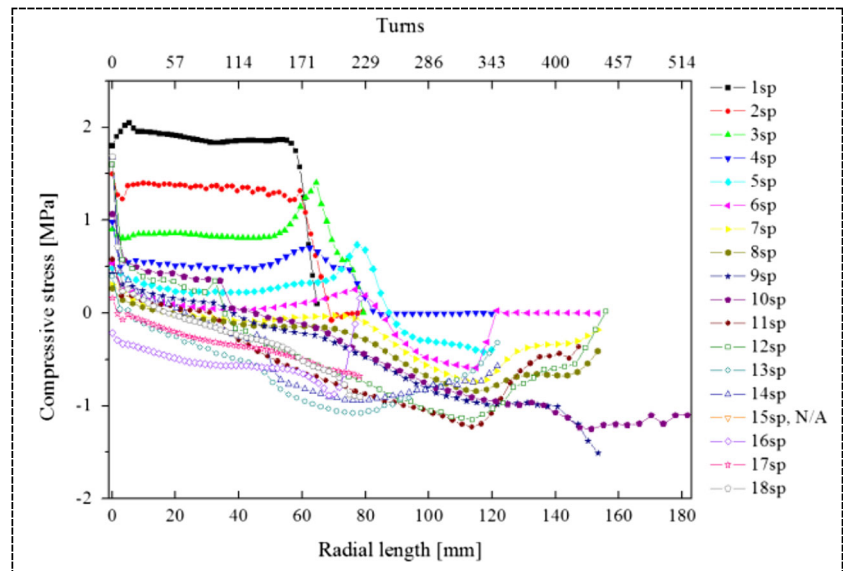


Fig. 8 Compressive-stress variation at the generated maximum compressive stress in the radial direction along the curvature of each SP coil; compression (+)



occurs in the 1st winding of the SP coil of the 6th layer, has a magnitude of 1.4 MPa. Finally, the maximum compressive stress is 2 MPa, as measured in the 16th winding of the SP coil of the 1st layer.

2.3 Analysis of the Mechanical Characteristics of the Rotor

The propulsion motor used in an electric propulsion system rotates at a low rotational speed of approximately 200 rpm. Therefore, a structural design with a stable stress distribution that does not exceed the allowable stress (yield strength) of the materials used is required because a high torque acts on the rotor of a motor compared with equivalent capacity.

Table 4 Mechanical stress along the curvature of the coil

Stress type	Direction of stress	Layer	Angle [°]	Value [MPa]	Turns
Maximum radial stress	Tension (+)	5 SP	60	2.7425	1
	Compression (-)	3 SP	74	2.6086	1
Maximum hoop stress	Tension (+)	6 SP	40	1.3844	1
	Compression (-)	6 SP	41	0.8687	1
Maximum comp. stress	Tension (+)	1 SP	29	2.0499	16
	Compression (-)	1 SP	42	2.0003	16

Equation (4) was used to design the rigidity of the rotating shaft, and the maximum torsional stress generated in the rotating shaft with the rotational torque is calculated by the torsion formula expressed in (4) [6]:

$$\varphi = \frac{T \cdot l}{G \cdot I_p} [\text{rad}] \tag{4}$$

$$\tau_{\text{max}} = \frac{T \cdot l}{I_p} [\text{MPa}] \tag{5}$$

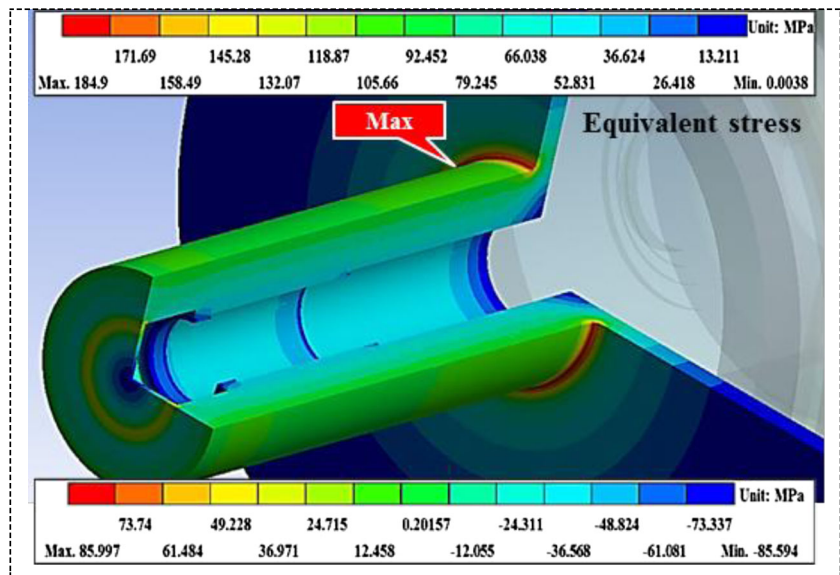
where φ is the torsion angle, T is the rated torque [N m], l is the length of the rotating shaft, G is the shear modulus of the material used, and I_p is the polar moment of inertia [m⁴]. Additionally, I_p depends on the cross-sectional shape of the rotating shaft and is $\pi d^4/32$ and $\pi(d_o^4 - d_i^4)/32$ for solid and hollow shafts, respectively, where d_o is the outer diameter of the rotating shaft, and d_i is the inside diameter of the rotating shaft. In designing the rotating shaft, the source side of the rotating shaft, which simultaneously transmits the torque and acts a cooling channel, was designed as a hollow

Table 5 Material properties for structural safety analysis

Material	SCM440	G10
Mass density [kg/m ³]	8030	1993
Young’s modulus [GPa]	204	34*
Poisson’s ratio	0.29	0.19*
Yield strength [MPa]	833	280
Shear yield strength [MPa]	568.4	N/A

*Warp direction @ 77 K

Fig. 9 Maximum equivalent stress of the hollow shaft in the rated load state



shaft. Additionally, the load side of the rotating shaft, which is directly connected to the load with a strong torsional moment, was designed as a solid shaft in order to enhance the rigidity of the rotating shaft.

Table 5 lists the properties of the materials used in the structural analysis of the rotor. SCM440 with a superior mechanical strength was used in the rotating shaft to withstand the frequent load changes. Moreover, the FRP with a low thermal conductivity, light weight, and high strength was used for the torque tube in order to maintain a stable operating temperature [8].

The equivalent-stress analysis results used to determine the structural safety of the rotating shaft for the HTS motor are presented in Fig. 9, and Table 6 lists the maximum value of each stress that occurs in the solid and hollow shaft

according to each load condition. At the rated load condition, the maximum equivalent stress occurs in the coupling part connected to the rotating shaft and flange, which is the most vulnerable part when the HTS motor rotates. The maximum equivalent stresses in the solid and hollow shafts are 158.66 and 184.9 MPa, respectively. For the rated load condition, the maximum torsional stresses of the solid and hollow shafts are 66.35 and 85.997 MPa, respectively.

The stress analysis results of the rotating shaft for equivalent load conditions show that a hollow shaft experiences approximately 1.3 times more stress than the solid shaft, and the weight of the designed hollow and solid shafts are 2022.84 and 4068.4 kg, respectively. Therefore, a hollow rotating shaft design enables a motor design with a lighter weight and greater torsional rigidity than a solid shaft

Table 6 Mechanical stress change in the rotating shaft according to changes in the load state

Load state	Solid shaft			Hollow shaft		
	σ_{eq} [MPa]	σ_τ [MPa]	σ_P [MPa]	σ_{eq} [MPa]	σ_τ [MPa]	σ_P [MPa]
50 %	79.782	33.33	47.939	92.852	43.23	55.38
100 %	158.66	66.35	93.483	184.9	85.997	111.5
150 %	237.55	99.37	139.03	276.97	128.76	167.61
200 %	316.43	132.4	184.59	369.05	171.53	223.72

* σ_{eq} is the equivalent stress, σ_τ is the torsional stress, and σ_P is the principal stress

Table 7 Mechanical stress change in the torque tube according to changes in the load state

Load state	Torque tube			
	50 %	100 %	150 %	200 %
σ_{eq} [MPa]	8.9704	17.612	26.255	34.899
σ_τ [MPa]	2.0866	4.1713	6.2561	8.3408
σ_P [MPa]	5.0362	10.094	15.156	20.22

* σ_{eq} , σ_τ , and σ_P are the equivalent stress, torsion stress, and principal stress, respectively

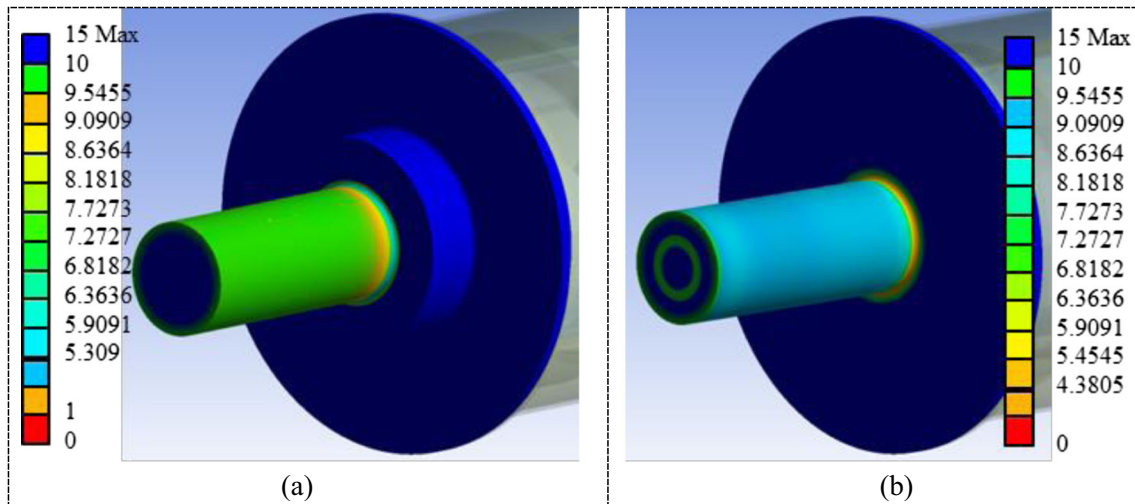


Fig. 10 Safety factor of (a) the solid shaft and (b) hollow shaft at twice the rated load

Table 7 summarizes the mechanical stress distribution that occurs in a torque tube according to the change in the load conditions. The maximum equivalent stress is 17.612 MPa at the rated load.

A safety factor, which determines whether or not damage and plastic deformation of the structure occur in the rotating shaft at each stage of the structural design, is expressed by (6)

$$S = \frac{\sigma_s}{\sigma_a} \quad (6)$$

where S , σ_s , and σ_a are the safety factor, basic strength, and allowable stress, respectively. The safety factor is defined as the ratio of the yield strength corresponding to the basic strength of the materials used to the allowable stress that can occur in the structures. If the value of the safety factor is greater than one, the structure will be safe from plastic deformation and fracture.

The safety factor for the rotating shaft that generates the greater mechanical stress in the rotor of a 17-MW-class HTS

motor for ship propulsion is shown in Fig. 10, and Table 8 lists the maximum and minimum values of each safety factor for the solid and hollow shafts according to the changes in each load condition. In the case where the hollow shaft has 70 % of the rigidity of the solid shaft, the hollow shaft has approximately four times greater structural rigidity at a torsional moment of 1.8 MN m at twice the rated load torque.

3 Conclusion

This paper discussed the structural safety of a 17-MW-class HTS synchronous motor that consists of HTS field coils and a rotor designed using a 3D FEA program.

From the mechanical-stress analysis results of the HTS field coils, the maximum equivalent stress evaluated from the calculated electromagnetic force was 7.46 MPa. Because this value is far below 270 and 40 MPa, which are the maximum yield strength of the Bi-2223 HTS wire in longitudinal

Table 8 Safety factor change in the rotating shaft according to changes in the load state

Load state	Solid shaft Safety factor		Hollow shaft Safety factor	
	Minimum	Maximum	Minimum	Maximum
50 %	15	15	15	15
100 %	10.483	15	8.7897	15
150 %	7.0485	15	5.847	15
200 %	5.309	15	4.3805	15

and transverse direction, respectively used in design, the structural safety is considered to be very good.

Additionally, the mechanical-stress analysis results of the rotor show that the maximum equivalent stress of the solid and hollow shafts, which were the most weakened parts mechanically, were 158.66 and 184.9 MPa, respectively. Because the stress analysis results show that the allowable stress of the materials used for the rotating shaft is 568.3 MPa, the rigidity margin of the rotating shaft could be confirmed by the mechanical-stress analysis results.

The stress analysis in this paper is the simplest first step for the structural design of a superconducting rotating machine. To ensure the structural safety of such a machine under actual conditions, we will study additional stress analyses considering the actual operating conditions including load changes and a cryogenic environment. Furthermore, these analysis results are quite helpful for future design research for optimizing HTS motors that will be applied to ship propulsion.

Acknowledgments This work was supported by the International Collaborative R&D Program and the Power Generation & Electricity Delivery of the Korea Institute of Energy Technology Evaluation and

Planning (KETEP) grant funded by the Korea government Ministry of Trade, Industry and Energy (NO. 20118520020020), (NO. 20113020020020)

References

1. Baik, S.K., et al.: Performance analysis of a superconducting motor for higher efficiency design. *IEEE Trans. Appl. Supercond.* **23**(3) (2013)
2. Kim, J.H., et al.: Magnetic field analysis of the field coil for 10 MW class superconducting wind turbines. *Supercond. Cryog.* **14**(3) (2012)
3. Kim, S.B., et al.: A study on electromagnetic and mechanical characteristics of the field coil in HTS motor. *Phys. C* **470**(20) (2010)
4. Handbook of Superconductivity, pp. 577–592. Department of Physics and Institute of Superconductivity, University of South Carolina, San Diego (2000)
5. Holtz, R.L., et al.: Transverse mechanical properties of BSCCO/Ag multifilamentary tapes. *IEEE Trans. Appl. Supercond.* **11**(1) (2001)
6. Gere, J.M., Goodno, B.: *Mechanics of Materials*. CENGAGE Learning Korea Ltd., Mapo-Ku (2011)
7. Kim, K.M., et al.: Stress analysis for toroid-type HTS SMES coil and bobbin structure considering large parallel magnetic field. *IEEE Trans. Appl. Supercond.* **21**(3) (2011)
8. Handbook of Applied superconductivity, vol. 2, p. 1020, Institute of Physics Publishing, Bristol and Philadelphia (1998)